STM JOURNALS

Research & Reviews: A Journal of
Pharmaceutical Science

ISSN: 2229-7006
Volume 15, Issue 2, 2024
May–August
DOI (Journal): 10.37591/RRJoPS

https://journals.stmjournals.com/rrjops

Review RRJoPS

Targeting Dystrophin Restoration and Neuroprotection in Duchenne Muscular Dystrophy: Insights from *Withania somnifera*

Siddhartha Pandurangi*

Abstract

Duchenne muscular dystrophy is a genetic disorder. This disease affects men more common than women. Main objective of the present study was to identify the naturally active phytocompounds from Withania somnifera (Ashwagandha). Ashwagandha has a great value in the field of Ayurveda and Indian medicine and is used for treating muscular and neurological disorders. Toxicity prediction, molecular docking, statistical information, drug illness prediction, and Absorption, distribution, metabolism, excretion, and toxicity analysis were used to predict the phytocompounds as a drug. Protein Data bank database was used to retrieve the Dystrophin protein and its chains. The poor binding affinity of the ligands with the targeted protein was removed. Toxicity and ADME analysis were done using ADMET lab 2.0 and Swiss ADME tools, respectively and molecular docking was done using PyRx. The Ramachandran plot displays the protein's dihedral angles ψ against φ. Absorption, distribution, metabolism, excretion, and toxicity analysis and molecular docking results showed Withaferine A, Somniferine, Coagulin Q, Physagulin D, Viscosalactone B have effective binding affinity towards Dystrophin protein and possess the properties of a drug which is safe to consume. Previous and present studies suggested that Withaferine A, Somniferine, Coagulin Q, Physagulin D, and Viscosalactone B could inhibit the A, B, C, and D chains of the Human Dystrophin protein and have effective binding affinity. The therapeutic strategies against Duchenne Muscular Dystrophy are based on molecular docking and ADMET analysis. Thus, the phytocompounds of Ashwagandha can be potential drug candidates.

Keywords: Duchenne muscular dystrophy, *Withania somnifera*, absorption, distribution, metabolism, excretion, and toxicity analysis, molecular docking, Ramachandran plot

INTRODUCTION

Duchenne Muscular Dystrophy (DMD) is an X-linked hereditary neuromuscular disorder caused by defects and mutations in the dystrophin gene. It is characterized by the progressive degradation of skeletal, cadaverous, and cardiac muscle as well as muscular waste because dystrophin protein is absent [1–3]. Myotonic dystrophy, Duchenne, Becker's Muscular Dystrophy (BMD), limb-girdle, facioscapulohumeral-humeral, congenital, oculo-pharyngeal, distal and Emery-Dreifuss are the main types of muscular dystrophy [4, 5]. One of the main goals of the treatment is to extend walking. Analyzing deletions and duplications using quantitative techniques such as microarray-based Comparative Genomic Hybridization (array-CGH) and Multiple Ligation Probe Assay (MLPA) is necessary for the molecular diagnosis of DMD [1].

About 10.2 live male births out of 100,000 are affected. A number of special care centers have

***Author for Correspondence**
Siddhartha Pandurangi
E-mail: siddhartha.pandurangi@gmail.com

Student, Department of Biotechnology, M.S. Ramaiah University of Applied Sciences, Bengaluru, Karnataka, India

Received Date: May 10, 2024
Accepted Date: June 14, 2024
Published Date: July 19, 2024

Citation: Siddhartha Pandurangi. Targeting Dystrophin Restoration and Neuroprotection in Duchenne Muscular Dystrophy: Insights from *Withania somnifera*. Research & Reviews: A Journal of Pharmaceutical Science. 2024; 15(2): 64–84p.

failed as a result of growing frequency of disease in young children. This genetic defect results from a sudden mutation or the absence of the muscle protein called Dystrophin (locus Xp 21.2) [2]. Dystrophin genes have a high mutation rate as compared to other human genes with about 2/3 of mutations being inherited and the remaining 1/3 of them occurring *de novo*. Mutations can be deletions (65%), duplications (9%), small mutations (25%), and rarely (<1%) atypical mutations. Genetic diagnosis of dystrophinopathies is complex and mutation identification is currently compulsory both for appropriate care, including prevention, and for eligibility to clinical trials and personalized treatments [4]. Following birth, the presentation sequence begins with somewhat delayed milestones throughout the toddler stage, which frequently include toe walking, trouble getting off the ground, and frequent falls and stumbling. There is a noticeable gap between surrounding classmates' physical abilities by the time the child becomes 5 years old. Respiratory, cardiac, and orthopedic involvement occur in second decade of life and reduce life expectancy (at the age of 18–20 years) in the absence of medical intervention. According to *Ayurveda*, a disease cannot be directly linked to any particular disease entity. This pathophysiology may be explained by the idea of *Adibala Pravritta Vyadhi* as it results from *beejadusti* and *anatman* or *karma* (self-deeds) which leads to *khavaigunya* of *mamsavahastrotas* causing phatagins impairment. When considering muscular dystrophy's gradual degeneration to systematic involvement, it may be viewed as an imbalance of *vatadosha, saptadhatu* (fundamental ingredients for creation of *Garbha*, both as functional and structural—to the level of *dhatwagni*) and *ojas*. A key characteristic is *chestahani*, or reduced movement, which denotes a decline in *chalaguna*. Both the medical and supportive sectors are continually revolutionizing life expectancy, resolving multi-systemic problems, and enhancing quality of life. *Ayurveda* states that the main principle for sustenance is the administration of medications with qualities such as *Medhya* (memory boosting), *Balya* (strengthening), *Rasayana* (rejuvenative), *Agnivardhana* (digestive and carminative), and *Vatadoshahara* followed by strengthening and revivification of *mamsadhatu* (muscle strengthening), both internally and externally. Muscle degeneration results from the stability and functionality of the muscle fibers being compromised by the lack of dystrophin. As of now, there is no proven cure for failing muscles or deteriorating muscles function in DMD patients. Gene transfer utilizing the safe, non-pathogenic Adeno Associated Viral (AAV) vector to restore dystrophin expression is a promising treatment opinion for this fatal illness. Even though large animal models of DMD have shown remarkably good treatment outcomes thus far using micro dystrophin gene transfer utilizing AAV vectors, there is still need for several optimization stages when bringing this advanced therapy medication from bench to bedside [2, 3]. Actin-binding domain (or N-terminal domain) of the dystrophin protein consists of four hinges (H1–H4), a rod domain, a C-terminal domain, 24 spectrin repeats (labeled R), and a cysteine-rich domain. The cysteine-rich domain, which binds dystroglycan, and the C-terminus which binds syntrophins and dystrobrevin, connect the extracellular matrix and internal cytoskeleton of dystrophin to the Dystrophin Associated Protein Complex (DAPC). The Neuronal Nitric Oxide Synthase (nNOS) binding sites found on R16 and R17 are crucial for nNOS localization in the sarcolemma [6–8].

Mechanism of Action of *Panchakarmas* on DMD

Abhyanga: It increases blood flow, vasodilation which nourishes and strengthens muscles, reduces thickening of connective tissue, and promotes flexibility by reducing fibrous adhesions from hypertrophied muscles. It has demonstrated a decrease in toe walking, reducing contractures, supporting muscle tone, nourishing atrophied muscles, and boosting muscle strength [9]. It has been shown that *Swedana*—Fomentation causes a decrease in gamma activity, which reduces the strain on muscle spindles and thus reduces muscular spasm. Increased muscle temperature can also change endurance and strength. Moreover, it leads to decrease in joint stiffness and increase in tissue elasticity, which promotes range of motion and comfort [10]. Considered as *bastyaupakarma, Virechana* has detoxification properties which enhance *Agni* and facilitate greater absorption of *bruhmana* and *rasayanadravya*.

Basti: Regarded as *gambhirdhatugatavikara*, to be ingrained as *karma* or *kaala basti* [11]. *Yapana basti* serves as both *lekhana* and *brumhana*. It is *medohara,* increases *Agni. Nasya* possesses the *Manaprasadana* action attribute [12]. It regulates the enteric nervous system (ENS).

Anuvasanabasti: It rejuvenates the body and further improves *dhatukshaya* (reduction of body tissue) [13].

MATERIALS AND METHODS

Selection and Preparation of the Target Protein

AutoDock is one of the most used tools for simulating receptor-ligand docking.

Since its first introduction in the early 1990s, it has undergone constant development and been tailored to target particular proteins. Applications for AutoDock have been implemented in several biological systems. It has been applied to the modeling of protein–ligand docking as well as the prediction of binding affinity for a number of protein systems showing a strong connection with experimental binding affinity [14]. The 3D structure of the target Human Dystrophin structural protein, N-terminal Actin-binding domain (Homo 2-mer) (PDB ID- IDXX), was downloaded in PDB format from RCSB Protein Data Bank Database (https://www.rcsb.org/). Visualization of the protein was done using the software Discovery Studio (BIOVIA) 2024 v24.1.0.23298.

Selection and Preparation of Ligand

The phytocompounds of *Withania somnifera* (leaf, root, seed) were extracted from IMPPAT database (https://cb.imsc.res.in/imppat/home) and were considered for molecular docking study. The 3D structure of all the 25 phytocompounds extracted were downloaded in structure data file (SDF) format from PubChem database (https://pubchem.ncbi.nlm.nih.gov/) and the top five ligands which showed best binding affinity score were selected. For making the macromolecule go to PyRx, click on file, and click on load molecule and open the cleaned dystrophin protein. Now right click on this option and click on 'AutoDock' and then make macromolecule. Now click on 'Open Babel' in the control panel and then click on 'add item' to select all the 25 phytocompounds one by one. Once all the phytocompounds are selected right click anywhere on the table and click on 'Minimize all.' Click "Convert all to AutoDock ligand (pdbqt format)" with a right-click once again. Select "Vina Wizard" from the control panel and press "Start." Now come towards the navigator panel and select one ligand, and press 'Ctrl key' and select all the remaining 24 ligands and click on 'forward' in the control panel. For flexible docking, click on 'Maximize' in the control panel for the protein to fit inside the box and click on forward. The results will be generated. Once the results are being generated, a tabular column appears in the control panel, click on retrieve the data in CSV format to analyze the results. Now select any five ligands which show the best binding affinity score for further studies. Go to navigator panel, click on AutoDock, and click on '+' symbol next to clean 1DXX. Now double click on the first ligand and download the respective model of ligand in ligand.pdb format. The same procedure is repeated for the remaining four ligands.

In silico Absorption, Distribution, Metabolism, and Excretion Analysis

The phytocompounds were assessed using Swiss ADME (http://www.swissadme.ch/) to conduct a pharmacokinetics research that included analyses of absorption, distribution, metabolism, extraction, and excretion.

The Canonical SMILES of the phytocompounds were obtained from PubChem database and pasted in Swiss ADME tool for ADME analysis. One stage in the medication development process is the evaluation of absorption, distribution, metabolism, and excretion (ADME). The Swiss ADME web tool offers free access to a pool of quick yet dependable predictive models for physicochemical qualities, pharmacokinetics, drug-likeness, and medicinal chemistry friendliness. This is made possible by in-house expert approaches such as the Brain Or IntestinaL EstimateD permeation method (BOILED-EGG), iLOGP, and Bioavailability Radar [15]. The computed physicochemical properties of compounds that successfully passed Phase I and entered Phase II clinical studies were correlated with their oral bioavailability, permeability, and aqueous solubility, according to a study by Lipinski and his colleagues. By doing this, the authors developed the "Rule of Five" —a memory aid that medicinal chemists can use to swiftly evaluate compounds in the course of drug discovery and optimization in

relation to the compounds' propensity to exhibit favorable permeability and solubility profiles [16] (Tables 1–14).

Table 1. Lipinski rule parameters [17, 18].

Property	Range
Molecular mass	< 500 Daltons
ClogP	≤ 5
Molar refractivity	40–130
Hydrogen bond donors	≤ 5
Hydrogen bond acceptors	≤ 10
Partition coefficient (logP)	-0.4 to +5.6
Polar surface area	≤ 140 A^{*2}

Physicochemical Properties

The molecular weight, Topological Polar Surface Area (TPSA), Lipophilicity (xLogP), flexibility, saturation (fraction Csp^3) was checked in physicochemical properties.

Protein Statistics and Ramachandran Plots

The FASTA files of human dystrophin protein were extracted from NCBI website (https://www.ncbi.nlm.nih.gov/), PDBsum, and PROCheck were used to build the Ramachandran plot for the protein. The FASTA files of human dystrophin protein were pasted in EMBOSS Pepwindow tool to obtain the Hydropathy plot and EMBOSS Pepstats tool was used to obtain the protein statistics, mole percentage, and residues.

Toxicity Prediction

The highly popular ADMETlab webserver has undergone a complete redesign. It is now called ADMETlab 2.0 (https://admetmesh.scbdd.com/service/screening/index) and it supports approximately twice as many as ADMET-related endpoints as the previous version did. These endpoints consist of eight toxicophoric rules (751 substructures), 27 toxicity endpoints, 13 medicinal chemistry properties, 23 ADME properties, and 17 physicochemical features. A multitask graph attention architecture was employed in ADMETlab 2.0 to generate accurate and dependable models. The batch computation module was made available in response to numerous customer requests, and the results' presentation was further enhanced [19]. The toxicity of the phytocompounds was predicted by pasting the Canonical SMILES into the tool and the data was retrieved in CSV format. The median lethal dose (LD_{50}) was categorized into four classes based on their level of toxicity.

Table 2. Toxicity categorization [20].

Class	LD_{50}(mg/kg)
I	LD_{50} <5
II	5< LD_{50} <50
III	50< LD_{50} <300
IV	300< LD_{50} <2000

RESULTS

Selection of Phytocompounds

A total of 25 phytocompounds of *W.somnifera* were extracted from IMPPAT database for molecular docking and virtual screening. Out of 25, only five compounds and their ligands showing best binding affinity towards the targeted dystrophin protein were selected.

Protein Structure Analysis

The three classes of dystrophin-associated proteins are extracellular (α-dystroglycan), transmembrane (β-dystroglycan, sarcoglycans, sarcospan), and cytoplasmic (dystrophin, dystrobrevin,

syntrophins, neuronal nitric oxide synthase), depending on where they are found in the cell. Sarcolemma's extracellular surface is home to α-dystroglycan because of its association with peripheral membranes and heavy glycosylation. A solitary transcript is translated into α-dystroglycan and β-dystroglycan, and the resulting peptide undergoes proteolytic processing to yield two distinct proteins [21]. In line with dystrophin glycoprotein complex (DGC's) function in muscle cell adhesion to the basal lamina, α-dystroglycan acts as a receptor for extracellular ligands such as laminin. The transmembrane protein—β-dystroglycan which also interacts with dystrophin—is closely linked to α-dystroglycan. α-dystroglycan is one of the few proteins that undergoes O-glycosylation or glycosylation on serine residues, and mutations in genes encoding a series of enzymes involved in glycosylation of α-dystroglycan (POMT1, POMT2, POMGnT1, FKTN, FKRP) resulting in LGMD2I, K, M, N and O [22]. Furthermore, mutations in human *LARGE, GTDC2, B3GNT1, POMK, GMPPB, and ISPD* genes have been shown to cause a wide spectrum of congenital muscular dystrophy by disrupting α-dystroglycan glycosylation pathway [23–28].

Table 3. Dystrophin protein statistics.

Molecule	Chains	Sequence length	Organism	Details
Dystrophin	A, B, C, D	246	*Homo sapiens*	Mutations:2 Gene names: *DMD*

Protein Statistics

The protein statistics were useful for the purification of protein and further research. The molecular weight of protein is 15369.48, total number of residues in the protein is 130, average residue weight of the protein is 118.227, charge obtained is -7.0 and isoelectric point is 4.6246. The property of amino acids, mole percentage and their numbers were obtained using the tool EMBOSS Pepstats (https://www.ebi.ac.uk/jdispatcher/seqstats/emboss_pepstats).

The hydropathy plot of the protein was obtained using EMBOSS Pepwindow (https://www.ebi.ac.uk/jdispatcher/seqstats/emboss_pepwindow) (Figure 1).

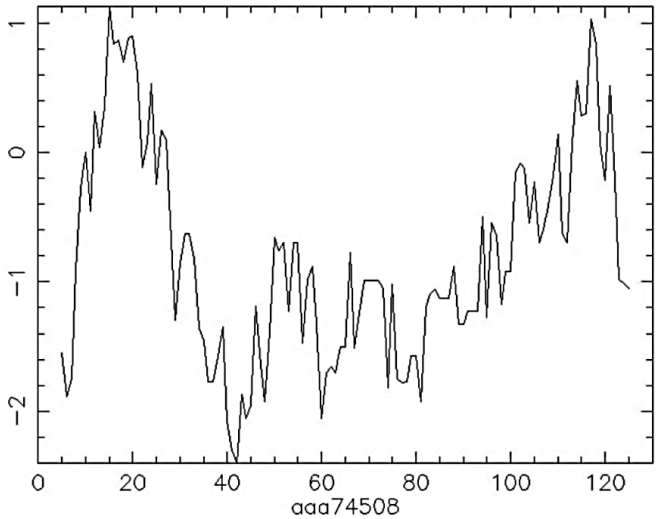

Figure 1. Hydropathy plot of human dystrophin protein.

Ramachandran Plot

When examining the energetically permitted regions for backbone dihedral angles ψ against φ of amino acid residues in protein structure, one can use a Ramachandran plot (Figure 2). To construct Ramachandran plot, we used tools named PDBsum and PROCheck (https://www.ebi.ac.uk/thornton-srv/databases/cgi-bin/pdbsum/GetPage.pl?pdbcode=1dxx&template=procheck_summary.html).

Table 4. Protein statistics, residues, and mole percentage.

Properties	Residues	Number	Mole%
Tiny	(A+C+G+S+T)	21	16.154
Small	(A+B+C+D+G+N+P+S+T+V)	44	33.846
Aliphatic	(A+I+L+V)	39	30.000
Aromatic	(F+H+W+Y)	8	6.154
Non-polar	(A+C+F+G+I+L+M+P+V+W+Y)	55	42.308
Polar	(D+E+H+K+N+Q+R+S+T+Z)	75	57.692
Charged	(B+D+E+H+K+R+Z)	50	38.462
Basic	(H+K+R	22	16.923
Acidic	(B+D+E+Z)	28	21.538

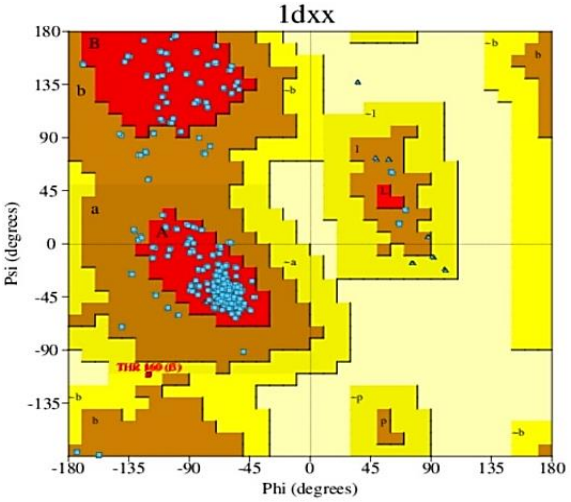

Figure 2. Ramachandran plot of human dystrophin protein.

The plot statistics observed 876 non-glycine and non-proline residues from a total of 952 residues. The plot displays the most preferred sections, A, B, and L, with 771 residues (88%) in red. Additionally allowed regions are represented as a, b, l, p with 115 residues (11.5%) indicated in brown color. Generously allowed regions are represented as ~a, ~b, ~l, ~p with four residues (0.5%) indicated in yellow color. Disallowed regions are represented as XX with no residues indicated in faint yellow color. The end residues will exclude eight Glycine and Proline residues.

Purification of Protein

The targeted human dystrophin protein was cleaned on Discovery Studio by deleting the heteroatoms. The cleaned protein was saved for further analysis and molecular docking (Figures 3 & 4).

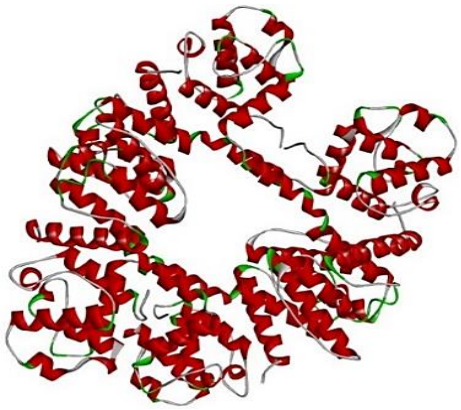

Figure 3. Purified dystrophin protein**.**

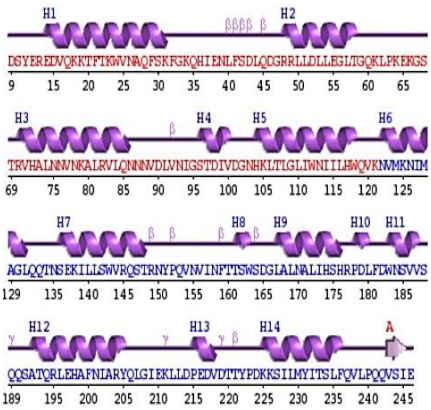

Figure 4. 2D structure of dystrophin protein.

Macromolecular Structure Analysis

The actin-binding amino-terminal domain (ABD1), central rod domain, cysteine-rich domain, and carboxyl-terminus are the four primary functional domains of dystrophin protein.

ABD1 contains two calponin homology disciplines (CH1 and CH2) [29, 30]. Dystrophin's central rod domain contains 24 spectrin repeats, which are ~110 aa motifs consisting of triple α-helices folded into small ~5 nm rods [31, 32]. Furthermore, a different set of spectrin repeats rich in basic amino acids are bridged by a second actin-binding motif (ABD2) located in the rod domain, suggesting that a connection with the acidic actin filaments is dependent on electrostatic interaction. [33]. It has also been demonstrated that the tryptophan residues in the spectrin-like repeats of dystrophin's rod bind membrane phospholipids *in vitro* [34]. In addition to dystrophin's association with F-actin, this interaction is assumed to further facilitate dystrophin's targeting of sarcolemma. Furthermore, the rod creates a flexible linker that connects the amino- and carboxy-termini. Four short proline-rich spacers are referred to as "hinges" because they provide elasticity to the protein break up at the 24 spectrin repeats [35]. The WW domain, which is present at the end of the rod domain and is involved in protein-protein interactions is found on hinge 4 [36]. The WW domain and two neighboring EF-hands bind the carboxy-terminus of β-dystroglycan, anchoring dystrophin at the sarcolemma. [37]. The EF-hand motifs are made up of two α-helices, connected by a brief loop region that has been connected to the binding of calcium [32].

The two EF-hands of dystrophin are found in the cysteine-rich domain, which is situated between the central rod and C-terminus. In addition to the cysteine rich domain, there is a zinc finger (ZZ) domain that folds to create a domain structure when divalent metal cations such as Zn^{2+} are present [38]. Dystrophin's ZZ domain attaches itself to calcium-dependent modulin [39]. It has also been demonstrated that the cysteine rich domain of dystrophin binds to ankyrin-B—an adaptor protein necessary for holding dystrophin at the sarcolemma [40]. Furthermore, it has been demonstrated that the rod's cysteine-rich domain and specific repeats bind to the intermediate filament protein synemin, enhancing the bond between costameric regions and myofibrils [41]. The spectrin repetitions in the rod domain are similar to the α-helical coiled coils formed by folding two polypeptides present in the CT domain [42]. Common protein motifs involved in protein–protein interaction are curled coils. Dystrobrevin and syntrophins binding sites are provided by the CT domain, which mediates the sarcolemma localization [43].

Table 5. Physicochemical properties.

Compound	Formula	MW	MlogP	H acceptors	H donors	MR
Hygrine	$C_8H_{15}NO$	141.21	0.76	2	0	45.47
Withanone	$C_{28}H_{38}O_6$	470.6	2.75	6	2	127.49
Withaferine A	$C_{28}H_{38}O_6$	470.6	2.75	6	2	127.53
Gamma-aminobutyric acid	$C_4H_9NO_2$	103.12	-0.39	3	2	25.82
Nicotine	$C_{10}H_{14}N_2$	162.23	1.17	2	0	53.13
Galactitol	$C_6H_{14}O_6$	182.17	-2.77	6	6	37.93
Tropine	$C_8H_{15}NO$	141.21	0.9	2	1	44.31
Pelletierine	$C_8H_{15}NO$	141.21	0.76	2	1	45.37
Cuscohygrine	$C_{13}H_{24}N_2O$	224.34	1.34	3	0	74.2
Scopoletin	$C_{10}H_8O_4$	192.17	0.76	4	1	51
Palmitic acid	$C_{16}H_{32}O_2$	256.42	4.19	2	1	80.8
Oleic acid	$C_{18}H_{34}O_2$	282.46	4.57	2	1	89.94
Linoleic acid	$C_{16}H_{32}O_2$	280.45	4.47	2	1	89.46
Beta-sitosterol	$C_{29}H_{50}O$	414.71	6.73	1	1	133.23
Somniferine	$C_{36}H_{36}N_2O_7$	608.68	1.67	9	2	171.39
Coagulin Q	$C_{34}H_{52}O_{10}$	620.77	1.25	10	6	161.86

Compound	Formula	MW	MlogP	H acceptors	H donors	MR
Physagulin-D	$C_{34}H_{52}O_{10}$	620.77	1.25	10	6	161.86
Hydrocortisone sodium succinate	$C_{25}H_{33}NaO_8$	484.51	1.29	8	2	116.72
Stigmasterone	$C_{29}H_{46}O$	410.67	6.53	1	0	131.79
Viscosalactone B	$C_{28}H_{40}O_7$	488.61	2.04	7	3	129.13
Beta-Amyrin	$C_{30}H_{50}O$	426.72	6.92	1	1	134.88
Esculetin	$C_9H_6O_4$	178.14	0.45	4	2	46.53
Fucosterol	$C_{29}H_{48}O$	412.69	6.62	1	1	132.75
Sominone	$C_{28}H_{42}O_5$	458.63	3.66	5	3	129.44
Daucosterol	$C_{35}H_{60}O_6$	576.85	3.96	6	4	165.61

MR: molecular refractivity; MW: molecular weight

Table 6. Physicochemical properties.

Compound	Fraction Csp_3	Rotatable bonds	TPSA	Lipophilicity
Hygrine	0.88	2	20.31	0.47
Withanone	0.79	3	96.36	3.83
Withaferine A	0.79	2	96.36	3.05
Gamma-aminobutyric acid	0.75	3	63.32	-3.17
Nicotine	0.5	1	16.13	1.17
Galactitol	1	5	121.38	-3.1
Tropine	1	0	23.47	0.75
Pelletierine	0.88	2	29.1	0.36
Cuscohygrine	0.92	4	23.55	1
Scopoletin	0.1	1	59.67	1.53
Palmitic acid	0.94	14	37.3	7.17
Oleic acid	0.83	15	37.3	7.64
Linoleic acid	0.72	14	37.3	6.98
Beta-sitosterol	0.93	6	20.23	9.34
Somniferine	0.47	3	100.93	2.61
Coagulin Q	0.85	5	166.14	2.47
Physagulin-D	0.85	5	166.14	2.47
Hydrocortisone sodium succinate	0.76	7	141.03	2.11
Stigmasterone	0.83	5	17.07	8.2
Viscosalactone B	0.86	3	116.59	2.85
Beta-Amyrin	0.93	0	20.23	9.15
Esculetin	0	0	70.67	1.22
Fucosterol	0.86	5	20.23	8.85
Sominone	0.82	3	86.99	4.72
Daucosterol	0.94	9	99.38	7.74

TPSA: topological polar surface area

PHARMACOLOGICAL STUDIES

ADME and BOILED-EGG Analysis

The molecules were plotted according to legends using BOILED-EGG analysis. Points located in the BOILED-Egg's yolk are molecules predicted to passively permeate through the blood–brain barrier, while points located in the BOILED-Egg's white are molecules predicted to be passively absorbed by gastrointestinal tract [29] (Figure 5).

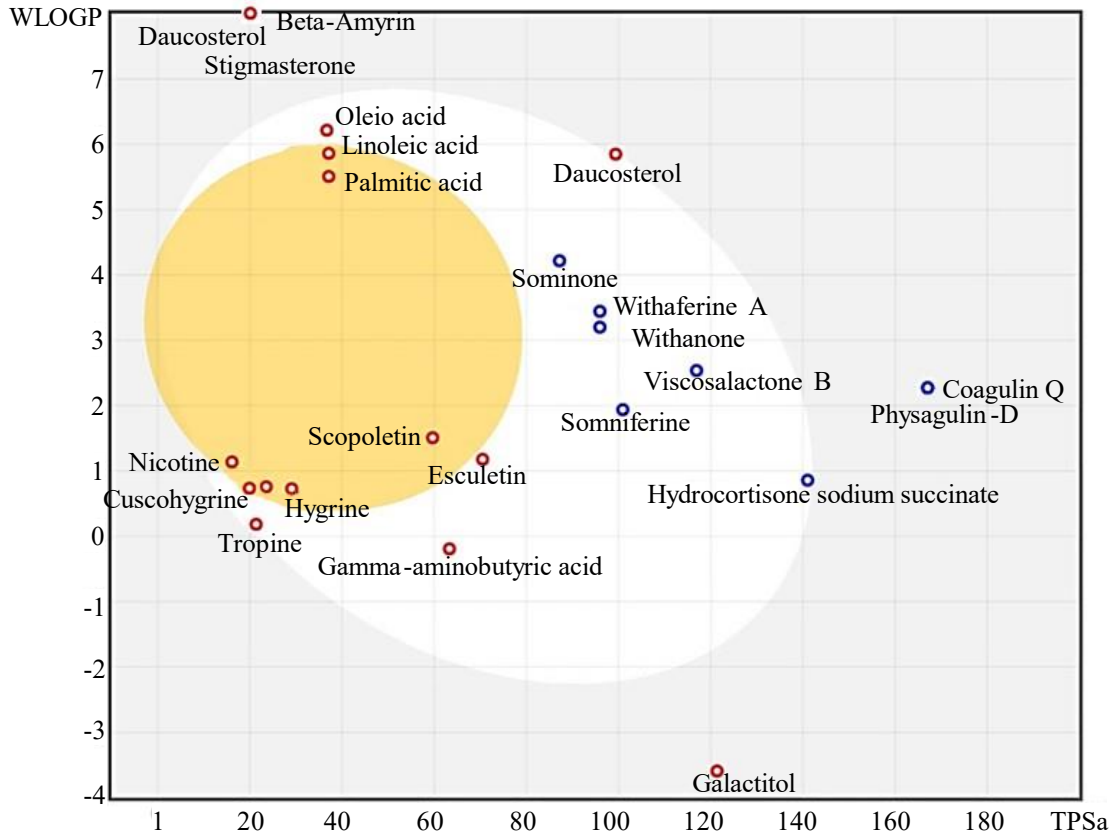

Figure 5. Brain Or IntestinaL Estimate D permeation predicted method (BOILED-EGG) analysis of the phytocompounds.

Table 7. ADME properties.

Compound	BBB permeant	GI absorption	PGP substrate	Solubility
Hygrine	No	High	No	-1.2
Withanone	No	High	Yes	-3.79
Withaferine A	No	High	Yes	-4
Gamma-aminobutyric acid	No	High	No	-0.04
Nicotine	Yes	High	No	-2.62
Galactitol	No	Low	No	2.57
Tropine	No	High	No	-0.25
Pelletierine	Yes	High	No	-1.8
Cuscohygrine	Yes	High	No	-1.85
Scopoletin	Yes	High	No	-3.17
Palmitic acid	Yes	High	No	-5.31
Oleic acid	No	High	No	-5.39
Linoleic acid	Yes	High	No	-4.67
Beta-sitosterol	No	Low	No	-6.19
Somniferine	No	High	Yes	-6.11
Coagulin Q	No	Low	Yes	-2.02
Physagulin D	No	Low	Yes	-2.02
Hydrocortisone sodium succinate	No	High	Yes	-2.99
Stigmasterone	No	Low	No	-6.17
Viscosalactone B	No	High	Yes	-3.44

Compound	BBB permeant	GI absorption	PGP substrate	Solubility
Beta-amyrin	No	Low	No	-7.16
Esculetin	No	High	No	-2.46
Fucosterol	No	Low	No	-5.83
Sominone	No	High	Yes	-3.84
Daucosterol	No	Low	No	-4.4

BBB: blood–brain barrier; GI: gastrointestinal; PGP: permeability glycophorin

Toxicity Predictions

Through the modulation of antioxidant pathways, *W.somnifera* has been demonstrated to prevent neurotoxic and neurodegenerative diseases.

Table 8. Toxicological properties.

Compound	LC_{50}	Carcinogenicity	Skin sensitivity	QEDw
Hygrine	2.485	0.782	0.73	0.573
Withanone	4.404	0.405	0.037	0.498
Withaferine A	3.732	0.338	0.011	0.364
Gamma-aminobutyric acid	2.56	0.12	0.261	0.52
Nicotine	3.024	0.235	0.918	0.626
Galactitol	-0.513	0.007	0.025	0.261
Tropine	2.261	0.434	0.875	0.534
Pelletierine	2.453	0.695	0.851	0.624
Cuscohygrine	2.459	0.821	0.709	0.723
Scopoletin	3.526	0.595	0.555	0.695
Palmitic acid	5.246	0.064	0.899	0.413
Oleic acid	4.794	0.084	0.951	0.291
Linoleic acid	5.113	0.153	0.961	0.318
Beta-sitosterol	5.365	0.047	0.133	0.436
Somniferine	7.067	0.834	0.825	0.545
Coagulin Q	6.107	0.049	0.007	0.198
Physagulin D	6.107	0.049	0.007	0.198
Hydrocortisone sodium succinate	3.134	0.694	0.016	0.555
Stigmasterone	5.468	0.068	0.049	0.419
Viscosalactone B	3.94	0.078	0.039	0.413
Beta-amyrin	6.786	0.017	0.035	0.387
Esculetin	4.108	0.721	0.921	0.469
Fucosterol	5.706	0.119	0.022	0.454
Sominone	4.68	0.208	0.068	0.437
Daucosterol	5.307	0.038	0.019	0.257

QEDw: weighted quantitative estimate of drug-likeness

Comparative studies investigating the antioxidant potential of different natural product formulations containing *W.somnifera* have shown the highest activity as compared to other formulations and standard ascorbic acid. It has demonstrated substantial (DPPH) free radical scavenging and hydrogen peroxide scavenging at 1000 g/ml and 100 g/ml concentrations, respectively. Besides being used as a neuroprotectant, the main impediment remains the blood brain barrier (BBB) penetrability of the active constituents of *W. somnifera.* There are no reports about the major Withanolides crossing the BBB. However, a single report in prevalent literature has shown that Withanamides (bioactive constituents

from fruit of *W. somnifera)* transverse the BBB after intraperitoneal administration of extract. Toxicological studies have found *W. somnifera* safe at very high doses in animals. In a study involving Wistar rats' hydro-alcoholic root extract of *W. somnifera* was found to have no toxicity even at higher dose of 2000 mg/kg body weight. During the acute toxicity study, treatment with 2000 mg/kg of the extract for 14 days and with 500 mg/kg, 1000 mg/kg, and 2000 mg/kg for 28 days for subacute toxicity test; no discernible alterations were observed in the body weight, organ weight, and haemato-biochemical parameters [44].

Molecular Docking Results

Ligand Retrieval

After analyzing the molecular docking results, the top five ligands which showed best binding interaction with the protein were selected and their respective models were downloaded in ligand.pdb format. The top five ligands which showed best binding interactions with the dystrophin protein were Withaferine A, Coagulin Q, Physagulin D, Somniferine, and Viscosalactone B (Figures 6–10).

Table 9. Binding affinity of the phytocompounds.

Compound	Binding affinity
Hygrine	-4.1
Withanone	-7.8
Withaferine A	-8.1
Gamma-aminobutyric acid	-4.1
Nicotine	-4.5
Galactitol	-4.8
Tropine	-4.4
Pelletierine	-4.6
Cuscohygrine	-4.9
Scopoletin	-5.6
Palmitic acid	-4.4
Oleic acid	-4.1
Linoleic acid	-4.2
Beta sitosterol	-6.9
Somniferine	-8.1
Coagulin Q	-8
Physagulin D	-8.1
Hydrocortisone sodium succinate	-7.2
Stigmasterone	-7.5
Viscosalactone B	-8
Beta-amyrin	-7.9
Esculetin	-5.7
Fucosterol	-7
Sominone	-7.6
Daucosterol	-7.7

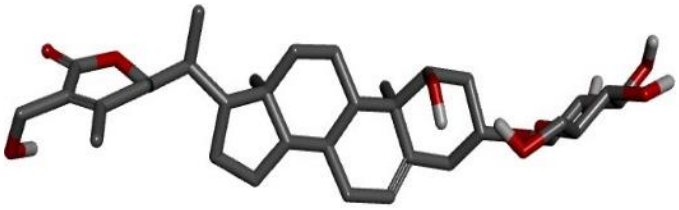

Figure 6. Ligand Withaferine A**.**

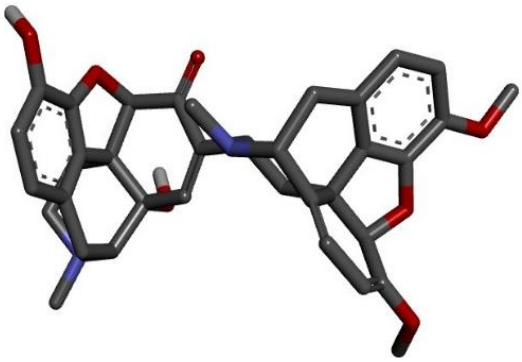

Figure 7. Ligand Somniferine.

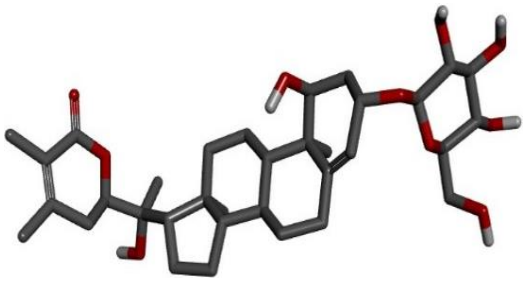

Figure 8. Ligand Coagulin Q.

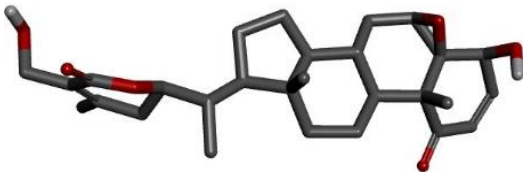

Figure 9. Ligand Physagulin D.

Figure 10. Ligand Viscosalactone B.

Docking of Protein with Selected Compound

After selecting the top five ligands which showed effective binding affinity towards the protein, and downloading their respective models in ligand.pdb format, Discovery Studio was used for further analysis of 2D interactions of the ligand and the protein. Open the clean 1DXX file and simultaneously open ligand 1(Withaferine A) file. Press Ctrl+H for the coordinate window of the ligand to appear. Click on ligand 1 in the coordinate window, copy it and paste it in the coordinate window of clean protein for the ligand to bind to the protein. Now in the tools section to define the ligand, click on ligand 1 in the coordinate window of the protein and then double click on 'define ligand-<undefined>' to define it. Now click on view 2D interactions to analyze the interaction between the ligand and protein complex. Repeat the same procedure for the remaining four ligands.

Visualization of Molecular Interaction of Withaferine A with Dystrophin Protein

The ligand was interacting with LEU 141, LYS 226, THR 160, THR 161, SER 142, LYS 138, and ASP 9 amino acids. The ligand Withaferine A had strong interactions with chains C and D of amino acids with binding affinity of -8.1 (Figures 11–15).

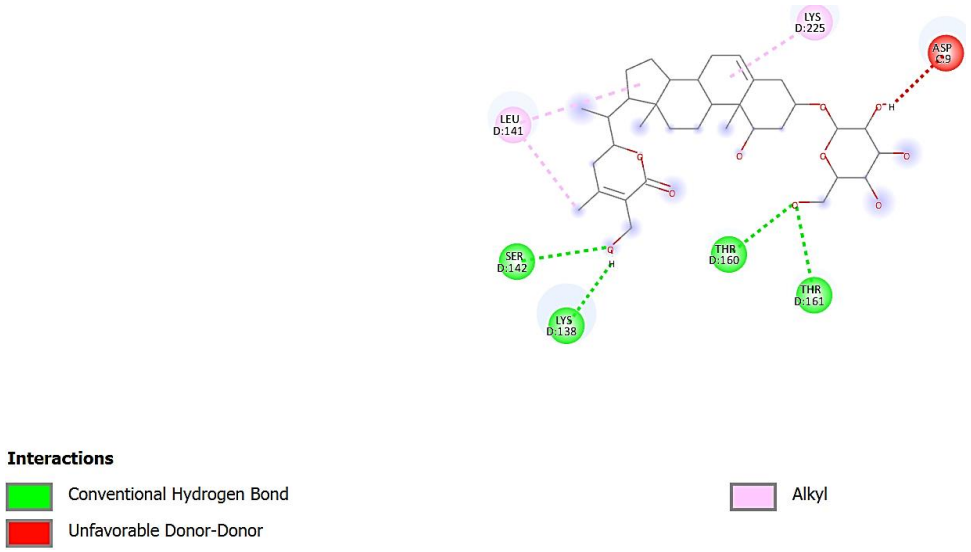

Figure 11. 2D interactions of ligand Withaferine A with Dystrophin protein

Table 10. 2D interactions of Withaferine A–protein complex.

Amino acid	Distance	Category	Type
D: LEU 141	4.02 and 4.84	Hydrophobic	Alkyl
D: LYS 225	4.85	Hydrophobic	Alkyl
D: THR 160	2.96	Hydrogen bond	Conventional hydrogen bond
D: THR 161	2.97	Hydrogen bond	Conventional hydrogen bond
D: SER 142	2.96	Hydrogen bond	Conventional hydrogen bond
D: LYS 138	2.89	Hydrogen bond	Conventional hydrogen bond
C: ASP 9	2.19		Unfavorable donor–donor

Visualization and Molecular Interaction of Somniferine with Dystrophin Protein

The ligand was interacting with SER 234, ILE 209, SER 30, and LYS 31 amino acids. The ligand Somniferine had strong interactions with chains C and D of amino acids with binding affinity of -8.1.

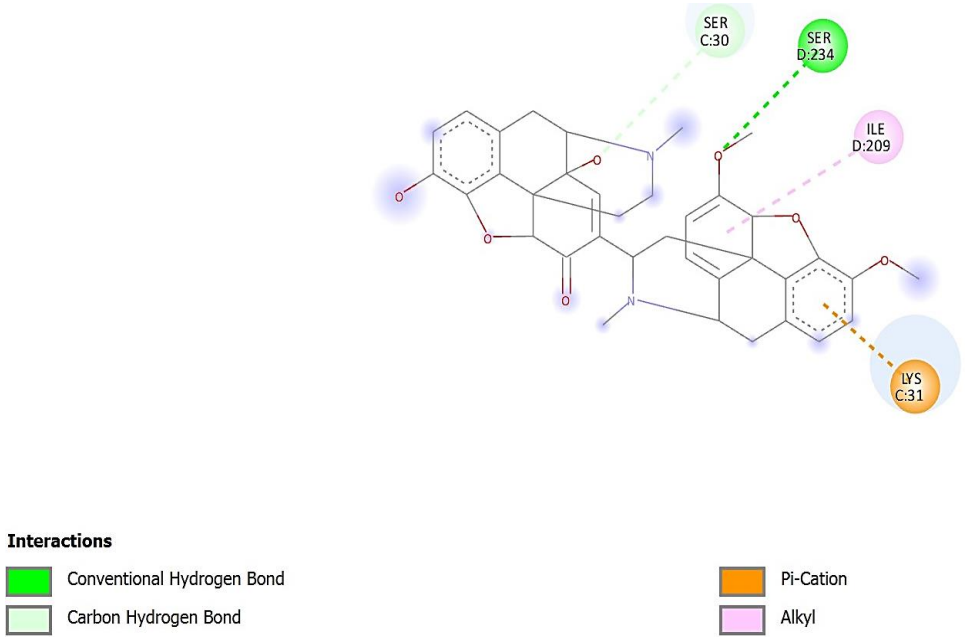

Figure 12. 2D interactions of ligand Somniferine with Dystrophin protein.

Table 11. 2D interactions of Somniferine–protein complex.

Amino acid	Distance	Category	Type
D: SER 234	2.89	Hydrogen bond	Conventional hydrogen bond
D: ILE 209	5.09	Hydrophobic	Alkyl
C: LYS 31	4.01	Hydrophobic	Pi-cation
C: SER 30	3.37	Hydrogen bond	Carbon hydrogen bond

Visualization and Molecular Interaction of Coagulin Q with Dystrophin Protein

The ligand was interacting with GLY 95, TRP 112, ASN 113, LYS 226, and GLU 12 amino acids. The ligand Coagulin Q had strong interactions with chains B, C and D of amino acids with binding affinity of -8.

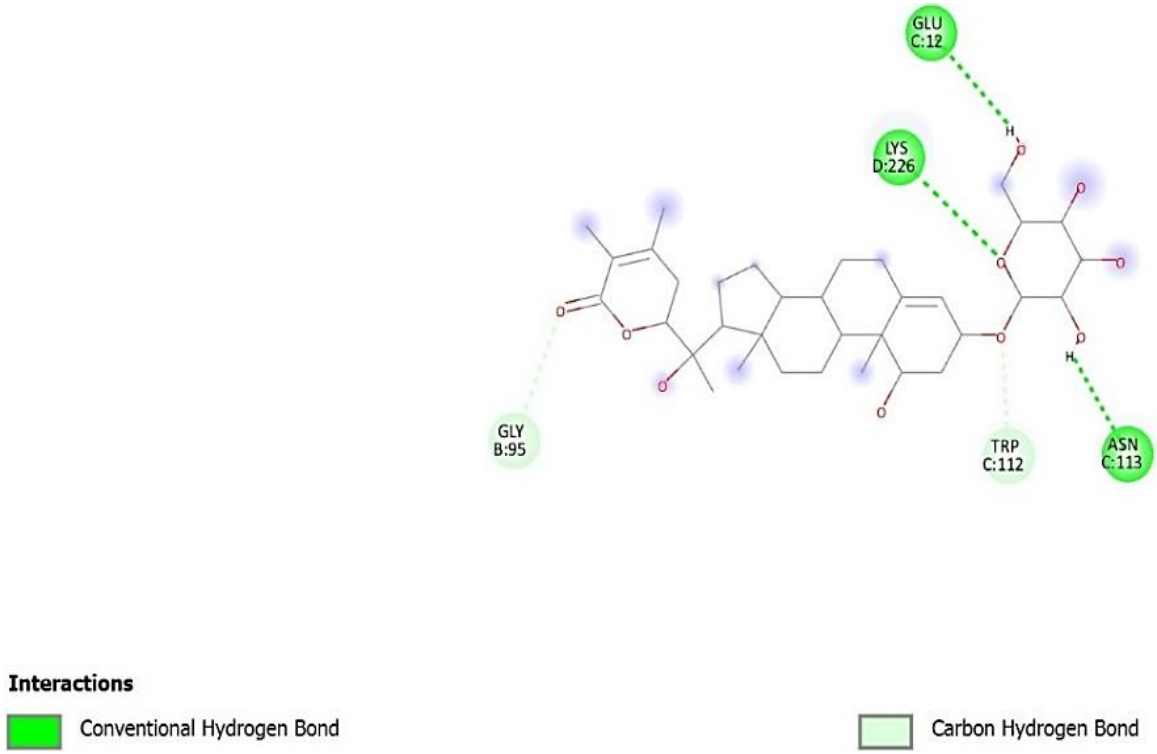

Figure 13. 2D interactions of ligand Coagulin Q with Dystrophin protein.

Table 12. 2D interactions of Coagulin Q-protein complex.

Amino acid	Distance	Category	Type
B: GLY 95	3.39	Hydrogen bond	Carbon hydrogen bond
C: TRP 112	3.49	Hydrogen bond	Carbon hydrogen bond
C: ASN 113	2.25	Hydrogen bond	Conventional hydrogen bond
C: GLU 12	2.65	Hydrogen bond	Conventional hydrogen bond
D: LYS 226	3.09	Hydrogen bond	Conventional hydrogen bond

Visualization and Molecular Interaction of Physagulin D with Dystrophin Protein

The ligand was interacting with ASN 155, ARG 149, ARG 145, SER 244, SER 244 amino acids. The ligand Physagulin D had strong interactions with chains A and B of the amino acids and showed a binding affinity value of -8.1.

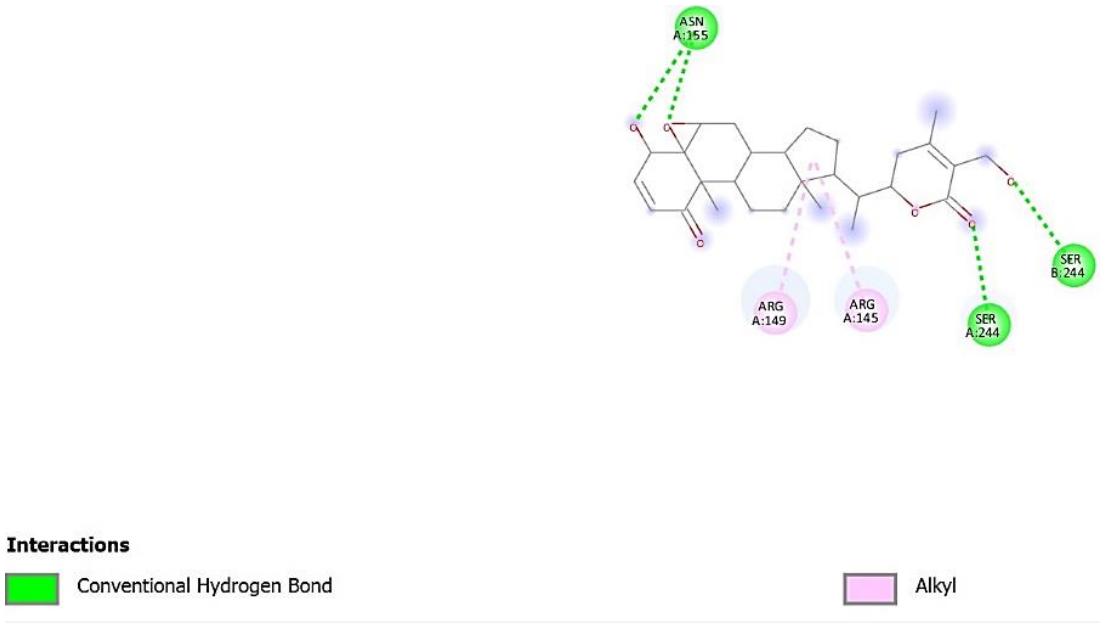

Figure 14. 2D interactions of ligand Physagulin D with Dystrophin protein.

Table 13. 2D interactions of Physagulin D-protein complex

Amino acid	Distance	Category	Type
A: ASN 155	2.88 and 3.01	Hydrogen bond	Conventional hydrogen bond
A: ARG 149	5.28	Hydrophobic	Alkyl
A: ARG 145	4.80	Hydrophobic	Alkyl
A: SER 244	3.03	Hydrogen bond	Conventional hydrogen bond
B: SER 244	2.98	Hydrogen bond	Conventional hydrogen bond

Visualization and Molecular Interactions of Viscosalactone B with Dystrophin Protein

The ligand was interacting with ASN 155, ARG 145, SER 244, SER 244, and ARG 149 amino acids. Viscosalactone B, the ligand, exhibited a binding affinity value of -8 and demonstrated robust interactions with amino acid chains A and B.

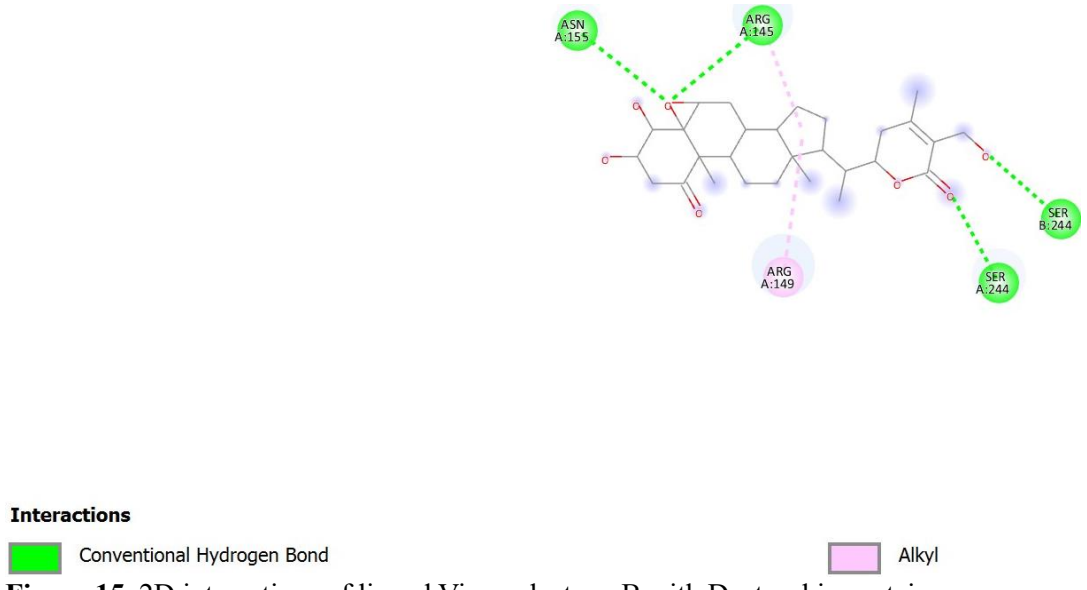

Figure 15. 2D interactions of ligand Viscosalactone B with Dystrophin protein.

Table 14. 2D interactions of Viscosalactone B–protein complex.

Amino acid	Distance	Category	Type
A: ASN 155	3.01	Hydrogen bond	Conventional hydrogen bond
A: ARG 145	3.30	Hydrogen bond	Conventional hydrogen bond
A: SER 244	3.06	Hydrogen bond	Conventional hydrogen bond
A: ARG 149	4.83 and 5.33	Hydrophobic	Alkyl
B: SER 244	2.87	Hydrogen bond	Conventional hydrogen bond

DISCUSSION

W. somnifera and its phytocompounds have antidiabetic, anti-epileptic, anti-inflammatory, anti-depressant, anti-arthritic, anti-cancer properties. *Ashwagandha* is an intriguing plant with a wide range of therapeutic properties that are being studied by researchers. While more research is needed to fully understand its benefits and dosages, *Ashwagandha* shows promise as a natural remedy for stress, inflammation, cognitive decline, and other health issues. Its capacity to raise testosterone levels and lower cortisol levels has also been demonstrated by studies.

Withaferin A, when given to albino rats with adjuvant-induced arthritis at a dose of 12–25 mg/kg of body weight, suppresses the arthritic syndrome without causing any adverse effects. In contrast to Hydrocortisone sodium succinate, Withaferine A caused animals with arthritic syndrome to gain more body weight. The findings demonstrated that Withaferine A is more effective than Hydrocortisone sodium succinate [45]. The plant's glycosides, specifically sitoindosides VII and VIII have been linked to anti-stress activity. Ashwagandha's value as an anti-stress adaptogen was supported by studies done by researchers [46]. The use of *W.somnifera* as a medicinal plant in *Ayurveda* as *Maharasayana* has recently been supported by scientific evidence as a cardioprotective agent [47–49]. It has been reported that *W. somnifera,* either in powder form or in combination with other medications, has a growth promoting effect. Withanolides are responsible for the increase in activity that promotes growth [50]. The effects of *Ashwagandha* roots on hypoglycemia and diuresis were also evaluated. Additionally noted were changes in urine volume, sodium, triglycerides, low density lipoproteins, and serum cholesterol [51]. Drugs derived from the roots of *W.somnifera,* such as Somniferine and Viscosalactone B, are used to treat epilepsy, rheumatic pain, and joint inflammation. Dried roots are used as a sedative, a tonic for female disorders, hiccups, cold, cough, and senile debility among other things. Leaves are used to treat swellings, inflammation, and carbuncles. Juice from the leaves can help with conjunctivitis. Its benefits include anti-inflammatory, antitumor, anti-stress, antioxidant, mind-boosting, immune-stimulating, and rejuvenating effects. There have also been reports of sex-enhancing qualities in its roots [52]. Its leaves are grounded into a paste that is used to treat tubercular gland inflammation. Fruits and seeds are diuretic in nature [53]. Condensed tannins, proteolytic enzymes, amino acids, and flavonoids are all present in green berries. The berries' high concentration of amino acids might be caused by the proteolytic enzyme chamase. The tender shoots are not fibrous and are high in phosphorous, calcium, and crude protein. Scopoletin is reportedly present in them. Numerous free amino acids are present in the bark [54]. It has been reported that Withaferine A and Withanolide D have strong antitumor and radio-sensitizing properties [55]. It has been reported that a different component of *W.somnifera,* 1-oxo-5ß, 6β-epoxy-witha-2-enolide, reduces skin carcinoma caused by UV radiation. It also inhibited colon, breast, lung, and central nervous system cancer cells by reducing their viability in a dose-dependent manner [56]. Withaferine A passed Lipinski's rule of 5 and had weighted quantitative estimate of drug-likeness (QEDw) value of 0.364. Somniferine passes Lipinski's rule of 5 and had QEDw value of 0.545. It was used for treatment of SARS-CoV-2 Coagulin Q passed Lipinski's rule of 5 and had QEDw value of 0.198. Physagulin D passed Lipinski's rule of 5 and had QEDw value of 0.198. Viscosalactone B, a Withanolide, passed Lipinski's rule of 5 and had QEDw value of 0.413. *Ashwagandha* is a better medicine for tiredness with nervous irritability because it is said to have a sedative rather than a stimulative effect on the central nervous system [57, 58].

CONCLUSION

W.somnifera is a natural product with promising pharmacological potential. In Indian systems of medicine, it has several preclinical and clinical uses. Through the modulation of PI3K/ Akt, MAPK signaling pathways, and anti-apoptotic cascades, extract from *W.somnifera* together with its active ingredients or metabolites have been shown in several cellular and animal models to contain antioxidant capabilities and rescue neuronal cells from toxic assaults and inflammation. Even though *Ashwagandha* has been effectively used for ages in *Ayurvedic* medicine, additional clinical research is needed to confirm its potential benefits. As a result, we may draw a conclusion that drugs such as Withaferine A, Somniferine, Coagulin Q, Physagulin D, and Viscosalactone B, which have lower toxicity levels and strong affinity for binding the dystrophin protein, may be suitable options.

Acknowledgement

I hereby acknowledge the Department of Bioinformatics, BioNome, Bengaluru, India for providing the necessary facilities and Ms. Samiksha Bhor for their guidance throughout the internship programme.

Funding

Nil

Abbreviations

Abbreviation	Full form
AAV vector	Adeno Associated Viral vector
ADMET	Absorption, Distribution, Metabolism, Excretion and Toxicity
BOILED-EGG	Brain Or IntestinaL EstimateD permeation predicted method
BBB	Blood Brain Barrier
BMD	Becker Muscular Dystrophy
CT domain	Carboxy terminal domain
Array-CGH	Comparative Genomic Hybridization
CSV	Comma Separated Values
DAPC	Dystrophin Associated Protein Complex
DMD	Duchenne Muscular Dystrophy
DGC	Dystrophin Glycoprotein Complex
ENS	Enteric Nervous System
FASTA	Fast Alignment Sequence Test for Application
GI tract	Gastrointestinal tract
IMPPAT	Indian Medicinal Plants, Phytochemistry and Therapeutics
LD	Lethal dose
MLPA	Multiple Ligation Probe Assay
MR	Molecular Refractivity
nNOS	Neuronal Nitric Oxide Synthase
NCBI	National Centre for Biotechnology Information
PDB	Protein Data Bank
PGP substrate	Permeability Glycophorin

QEDw	Weighted Quantitative Estimate of Drug-likeness
SDF	Structure Data File
SMILES	Simplified Molecular- Input Line-Entry System
TPSA	Topological Polar Surface Area

REFERENCES

1. Falzarano M, Scotton C, Passarelli C, Ferlini A. Duchenne muscular dystrophy: From diagnosis to therapy. Molecules. 2015; 20(10): 18168–18184p. Available from: http://dx.doi.org/10.3390/molecules201018168
2. Banik DS. A critical review on duchenne muscular dystrophy through Ayurveda–a practical approach. World J Pharm Res. 2017; 864–872p. Available from: http://dx.doi.org/10.20959/wjpr20178-9205
3. Elangkovan N, Dickson G. Gene therapy for duchenne muscular dystrophy. J Neuromuscul Dis. 2021; 8(s2): S303–S316. Available from: http://dx.doi.org/10.3233/jnd-210678
4. Fortunato F, Farnè M, Ferlini A. The DMD gene and therapeutic approaches to restore dystrophin. Neuromuscul Disord. 2021; 31(10): 1013–1020p. Available from: http://dx.doi.org/10.1016/j.nmd.2021.08.004
5. Jain M. Neuro-muscular diseases, Muscular dystrophies, Parkinson's disease, Autism, Cerebral Palsy and mentally challenged children. Sanjivni Wellness [Internet]; 2024.
6. Davies KE, Nowak KJ. Molecular mechanisms of muscular dystrophies: old and new players. Nat Rev Mol Cell Biol. 2006; 7(10): 762–773p. Available from: http://dx.doi.org/10.1038/nrm2024
7. Fairclough RJ, Wood MJ, Davies KE. Therapy for Duchenne muscular dystrophy: renewed optimism from genetic approaches. Nat Rev Genet. 2013; 14(6): 373–378p. Available from: http://dx.doi.org/10.1038/nrg3460
8. Duan D. Micro-dystrophin gene therapy goes systemic in duchenne muscular dystrophy patients. Hum Gene Ther. 2018; 29(7): 733–736p. Available from: http://dx.doi.org/10.1089/hum.2018.012
9. Chaturvedi A, Rao PN, Uppinakudru S, Kumar MA. Role of Panchakarma in Duchenne Muscular Dystrophy. Int J Res Ayurveda Pharm. 2013; 4(2): 272–275p. Available from: http://dx.doi.org/10.7897/2277-4343.04238
10. Sinha AG. Principles and Practice of Therapeutic massage, Edition. 243. New Delhi: Jaypee Brothers Medical Publishers; 2021.
11. Mukesh J, Annapurna Y, Pandey MP. Preliminary study of integrated approach of Panchakarma, Yoga & Ayurvedic medicine in the management of muscular dystrophy. World Health Review. 2002; 1: 1–33p.
12. Agnivesa C, Chakrapannidatta A. Charaka Samhita With Chakrapannidatta, Ayurveda Dipika. Commentary. Mumbai: Nirnaya Sagar Press; 2008. 731–732p.
13. Shailaja U, Rao PN, Girish KJ, Raj GRA. Clinical study on efficacy of Rajayapana Basti & Baladi Yoga in motor disabilities of cerebral palsy in children. Ayu. 2014; 35(3): 294–299p.
14. Bitencourt-Ferreira G, Pintro VO, de Azevedo WF Jr. Docking with AutoDock4. In: Methods in Molecular Biology. New York, NY: Springer New York; 2019. 125–148p.
15. Daina A, Michielin O, Zoete V. SwissADME: A free web tool to evaluate pharmacokinetics, drug-likeness and medicinal chemistry friendliness of small molecules. Sci Rep. 2017; 7(1): 42717. Available from: http://dx.doi.org/10.1038/srep42717
16. Pollastri MP. Overview on the Rule of Five. Curr Protoc Pharmacol. 2010; 49(1): 12.1–12.8. Available from: http://dx.doi.org/10.1002/0471141755.ph0912s49
17. Lipinski CA, Lombardo F, Dominy BW, Feeney PJ. Experimental and computational approaches to estimate solubility and permeability in drug discovery and development settings. Advanced Drug Delivery Reviews. 2001; 46(1–3): 3–26p. Available from: http://dx.doi.org/10.1016/s0169-409x(00)00129-0
18. Ghose AK, Viswanadhan VN, Wendoloski JJ. A knowledge-based approach in designing combinatorial or medicinal chemistry libraries for drug discovery. 1. A qualitative and quantitative

characterization of known drug databases. J Comb Chem. 1999; 1(1): 55–68p. Available from: http://dx.doi.org/10.1021/cc9800071
19. Dong J, Wang NN, Yao ZJ, Zhang L, Cheng Y, Ouyang D, et al. ADMETlab: a platform for systematic ADMET evaluation based on a comprehensively collected ADMET database. J Cheminform. 2018; 10(1): 29p. Available from: http://dx.doi.org/10.1186/s13321-018-0283-x
20. Schlede E, Genschow E, Spielmann H, Stropp G, Kayser D. Oral acute toxic class method: a successful alternative to the oral LD50 test. Regul Toxicol Pharmacol. 2005; 42(1): 15–23p. Available from: http://dx.doi.org/10.1016/j.yrtph.2004.12.006
21. Ibraghimov-Beskrovnaya O, Ervasti JM, Leveille CJ, Slaughter CA, Sernett SW, Campbell KP. Primary structure of dystrophin-associated glycoproteins linking dystrophin to the extracellular matrix. Nature. 1992; 355(6362): 696–702p. Available from: http://dx.doi.org/10.1038/355696a0
22. Nigro V, Savarese M. Genetic basis of limb-girdle muscular dystrophies: the 2014 update. Acta Myol. 2014; 33(1): 1–12p.
23. Buysse K, Riemersma M, Powell G, Van Reeuwijk J, Chitayat D, Roscioli T, et al. Missense mutations in beta-1,3-N-acetylglucosaminyltransferase 1 (B3GNT1) cause Walker-Warburg syndrome. Hum Mol Genet. 2013; 22: 1746–1754p.
24. Carss KJ, Stevens E, Foley AR, Cirak S, Riemersma M, Torelli S, et al. Mutations in GDP-mannose pyrophosphorylase B cause congenital and limb-girdle muscular dystrophies associated with hypoglycosylation of alpha-dystroglycan. Am J Hum Genet. 2013; 93: 29–41p.
25. Di Costanzo S, Balasubramanian A, Pond HL, Rozkalne A, Pantaleoni C, Saredi S, et al. POMK mutations disrupt muscle development leading to a spectrum of neuromuscular presentations. Hum Mol Genet. 2014; 23(21): 5781–5792p. Available from: http://dx.doi.org/10.1093/hmg/ddu296
26. Longman C, Brockington M, Torelli S, Jimenez-Mallebrera C, Kennedy C, Khalil N, et al. Mutations in the human LARGE gene cause MDC1D, a novel form of congenital muscular dystrophy with severe mental retardation and abnormal glycosylation of alpha-dystroglycan. Hum Mol Genet. 2003; 12(21): 2853–2861p. Available from: http://dx.doi.org/10.1093/hmg/ddg307
27. Ogawa M, Nakamura N, Nakayama Y, Kurosaka A, Manya H, Kanagawa M, et al. GTDC2 modifies O-mannosylated alpha-dystroglycan in the endoplasmic reticulum to generate N-acetyl glucosamine epitopes reactive with CTD110.6 antibody. Biochem Biophys Res Commun. 2013; 440: 88–93p.
28. Willer T, Lee H, Lommel M, Yoshida-Moriguchi T, de Bernabe DBV, Venzke D, et al. ISPD loss-of-function mutations disrupt dystroglycan O-mannosylation and cause Walker-Warburg syndrome. Nat Genet. 2012; 44(5): 575–580p. Available from: http://dx.doi.org/10.1038/ng.2252
29. Gomaa MS, Ali IAI, El Enany G, El Ashry ESH, El Rayes SM, Fathalla W, et al. Facile synthesis of some coumarin derivatives and their cytotoxicity through VEGFR2 and topoisomerase II inhibition. Molecules. 2022; 27(23): 8279p. Available from: http://dx.doi.org/10.3390/molecules27238279
30. Korenbaum E, Rivero F. Calponin homology domains at a glance. J Cell Sci. 2002; 115(18): 3543–3545p. Available from: http://dx.doi.org/10.1242/jcs.00003
31. Broderick MJF, Winder SJ. Spectrin, alpha-actinin, and dystrophin. Adv Protein Chem. 2005; 70: 203–246p. Available from: http://dx.doi.org/10.1016/S0065-3233(05)70007-3
32. Koenig M, Monaco AP, Kunkel LM. The complete sequence of dystrophin predicts a rod-shaped cytoskeletal protein. Cell. 1988; 53(2): 219–228p. Available from: http://dx.doi.org/10.1016/0092-8674(88)90383-2
33. Amann KJ, Renley BA, Ervasti JM. A cluster of basic repeats in the dystrophin rod domain binds F-actin through an electrostatic interaction. J Biol Chem. 1998; 273(43): 28419–28423p. Available from: http://dx.doi.org/10.1074/jbc.273.43.28419
34. Rumeur L, Fichou E, Pottier Y, Gaboriau S, Rondeau-Mouro F, Vincent C, et al. Interaction of dystrophin rod domain with membrane phospholipids. Evidence of a close proximity between tryptophan residues and lipids. J Biol Chem. 2003; 278: 5993–6001p.
35. Koenig M, Kunkel LM. Detailed analysis of the repeat domain of dystrophin reveals four potential hinge segments that may confer flexibility. J Biol Chem. 1990; 265(8): 4560–4566p. Available from: http://dx.doi.org/10.1016/s0021-9258(19)39599-7

36. Ilsley JL, Sudol M, Winder SJ. The WW domain: linking cell signalling to the membrane cytoskeleton. Cell Signal. 2002; 14(3): 183–189p. Available from: http://dx.doi.org/10.1016/s0898-6568(01)00236-4
37. Rentschler S, Linn H, Deininger K, Bedford MT, Espanel X, Sudol M. The WW domain of dystrophin requires EF-hands region to interact with beta-dystroglycan. Biol Chem. 1999; 380(4): 431–442p. Available from: http://dx.doi.org/10.1515/BC.1999.057
38. Ponting CP, Blake DJ, Davies KE, Kendrick-Jones J, Winder SJ. ZZ and TAZ: new putative zinc fingers in dystrophin and other proteins. Trends Biochem Sci. 1996; 21(1): 11–13p. Available from: http://dx.doi.org/10.1016/s0968-0004(06)80020-4
39. Anderson JT, Rogers RP, Jarrett HW. Ca^{2+}-calmodulin binds to the carboxyl-terminal domain of dystrophin. J Biol Chem. 1996; 271(12): 6605–6610p. Available from: http://dx.doi.org/10.1074/jbc.271.12.6605
40. Ayalon G, Davis JQ, Scotland PB, Bennett V. An ankyrin-based mechanism for functional organization of dystrophin and dystroglycan. Cell. 2008; 135(7): 1189–1200p. Available from: http://dx.doi.org/10.1016/j.cell.2008.10.018
41. Bhosle RC, Michele DE, Campbell KP, Li Z, Robson RM. Interactions of intermediate filament protein synemin with dystrophin and utrophin. Biochem Biophys Res Commun. 2006; 346(3): 768–777p. Available from: http://dx.doi.org/10.1016/j.bbrc.2006.05.192
42. Blake DJ, Tinsley JM, Davies KE, Knight AE, Winder SJ, Kendrick-Jones J. Coiled-coil regions in the carboxy-terminal domains of dystrophin and related proteins: potentials for protein-protein interactions. Trends Biochem Sci. 1995; 20(4): 133–135p. Available from: http://dx.doi.org/10.1016/s0968-0004(00)88986-0
43. Sadoulet-Puccio HM, Rajala M, Kunkel LM. Dystrobrevin and dystrophin: an interaction through coiled-coil motifs. Proc Natl Acad Sci U S A. 1997; 94(23): 12413–12428p. Available from: http://dx.doi.org/10.1073/pnas.94.23.12413
44. Dar NJ, Ahmad M. Neurodegenerative diseases and Withania somnifera (L.): An update. J Ethnopharmacol. 2020; 256(112769): 112769p. Available from: http://dx.doi.org/10.1016/j.jep.2020.112769
45. Rastogi RP, Mehrotra BN. Compendium of Indian medicinal plants, 2nd Reprint. Lucknow & New Delhi: Central Drug Research Institute and National Institute of Science Communication, Council of Scientific and Industrial Research; 1998.
46. Bhattacharya A, Ghosal S, Bhattacharya SK. Antioxidant effect of Withania somnifera glycowithanolides in chronic footshock stress-induced perturbations of oxidative free radical scavenging enzymes and lipid peroxidation in rat frontal cortex and striatum. J Ethnopharmacol. 2001; 74: 1–6p.
47. Nadkarni KM. Indian materia medica. Bombay: Popular Prakshan Limited; 1908. 1291p.
48. Lohar DR, Chaturvedi D, Varma PN. Mineral elements of a few medicinally important plants. Ind Drugs. 1992; 29: 271–273p.
49. Mohanty I, Arya DS, Dinda A, Talwar KK, Joshi S, Gupta SK. Mechanisms of Cardioprotective effect of Withania somnifera in experimentally induced myocardial infarction. Basic Clin Pharmacol Toxicol. 2004; 94(4): 184–190p.
50. Bilal Ahmad Mi J, Nisar A. Tanvir-ul Hasan, Sushma Koul, Botanical, chemical and pharmacological review of Withania somnifera (Indian ginseng): An ayurvedic medicinal plant. Indian Journal of Drugs and Diseases. 2012; 1(6): 147–160p.
51. Andulla B, Radhika B. Hypoglycemic, diuretic and hypocholesterolemic effect of winter cherry (Withania somnifera) root. Indian J Exp Biol. 2000; 38: 607–609p.
52. Battacharya SK. Adaptogenic activity of Withania somnifera an experimental study using a rat model of chronic stress. Journal of Pharmacological. 2003; 75(3): 547–555p.
53. Rani A, Baranwal NR, Nema RK. Pharmacognostical & Phytochemical studies of Withania somnifera. Asian Journal of Biochemical and Pharmaceutical Research. 2012; 2(4): 195–198p.
54. Qamar U, Samiulla L, Singh VK, Jamil S. Phytochemical and Pharmacological Profile of Withania somnifera Dunal: A Review. Journal of Applied Pharmaceutical Science. 2012; 2(1): 170–175p.

55. Devi PU, Sharada AC, Solomon FE. Antitumor and radiosensitizing effects of Withania somnifera (ashwagandha) on a transplantable mouse tumor, Sarcoma-180. Ind. J Exp Biol. 1993; 31: 607–611p.
56. Davis L, Kuttan G. Suppressive effect of cyclophosphamide-induced toxicity by Withania somnifera extract in mice. J Ethnopharmacol. 1998; 62(3): 209–214p. Available from: http://dx.doi.org/10.1016/s0378-8741(98)00039-7
57. Malhotra CL, Mehta VL, Das PK, Dhalla NS. Studies on Withania-ashwagandha, Kaul. V. The effect of total alkaloids (ashwagandholine) on the central nervous system. Ind J Physiol Pharmacol. 1965; 9: 127–136p.
58. Sehgal N, Gupta A, Khader R, Shanker V, Joshi D, Mills JT, et al. Withania somnifera reverses Alzheimer's disease pathology by enhancing low-density lipoprotein receptor-related protein in liver, Proc. Proc Nat Acad Sci. 2012; 109(9): 3510–3515p.

